Sustainable Grafting of (Ligno)Cellulose-Based Powders with Antibacterial Functionalities: Effect of Biomass Type and Synthesis Conditions

Maria Luisa Testa, Omar Ginoble Pandoli, Claudio Cecone, Enzo Laurenti, Valeria La Parola, Claudia Vineis, and Maria Laura Tummino*

The problem of microbial resistance to antibiotics makes it necessary to develop new materials capable of overcoming the resistance to the chemicals currently used. Herein, the antibacterial properties of modified bamboo powder are tested and compared with modified cellulose isolated from soybean hulls. Such biomasses are functionalized in a water solution with (3-aminopropyl)triethoxysilane to introduce primary amino groups, and two different functionalization procedures are adopted: the first requires conventional heating steps, whereas the second implies microwave radiation use. The main outcomes from the characterizations evidence that the materials prepared with the thermal treatment are stabler than those obtained by the microwave-assisted procedure and that bamboo-derived samples react with the (3-aminopropyl)triethoxysilane through different functionalities other than hydroxyl groups. Finally, the antibacterial activity measured against *Escherichia coli* and *Staphylococcus aureus* shows that all the functionalized samples could efficiently remove Gram-positive and Gram-negative bacteria (removal > 93%). Moreover, active filters are realized by packing the material powders: when the bacterial inoculum passes through them in a continuous flow, some differences are observed between cellulose and bamboo-based materials, but the overall performances show that after 17 min and five recirculation cycles, both the samples reach an excellent *Escherichia coli* removal of about 100%.

1. Introduction

The development of innovative antibacterial materials different from traditional antibiotics attracts much attention due to the intensification of antimicrobial resistance by several microorganisms that can cause sanitary crises, as witnessed by several sources and debated both in the research field and among policymakers[1,2] (see, for instance, Goal 3 "Ensure healthy lives and promote well-being for all at all ages" of the United Nations' Sustainable Development Goals). Many antibacterial agents on the market are produced from inorganic (such as metal nanoparticles) and nonrenewable substances. Moreover, commonly used disinfectant chemicals such as hydrogen peroxide and chlorine-based compounds are even more often insufficient to fight microorganisms.[3] In order to improve efficiency and promote the transition toward the use of renewable materials, the research is oriented toward the development of renewable antibacterial materials, such as biomass-derived ones.[4] This trend is also favored by the global and urgent necessity of reconsidering the productive paradigms in all the industrial sectors (biomedical, energy supply, construction, environment remediation, etc.) where biomass, better if wasted, can be exploited as a sustainable carbon-based raw material, often substituting fossil resources.[5–9] These greener strategies are again promoted among the United Nations'

M. L. Testa, V. La Parola
Institute for the Study of Nanostructured Materials (ISMN)
Italian National Research Council (CNR)
Via U. La Malfa 153, Palermo 90146, Italy

O. G. Pandoli
Department of Pharmacy
University of Genova
Viale Cembrano 4, Genova 16147, Italy

C. Cecone, E. Laurenti
Department of Chemistry
University of Torino
Via P. Giuria 7, Torino 10125, Italy

C. Vineis, M. L. Tummino
Institute of Intelligent Industrial Technologies and Systems for Advanced Manufacturing (STIIMA)
Italian National Research Council (CNR)
Corso G. Pella 16, Biella 13900, Italy
E-mail: marialaura.tummino@cnr.it

**ADVANCED
SCIENCE NEWS**

www.advancedsciencenews.com

**ADVANCED
SUSTAINABLE
SYSTEMS**

www.advsustainsys.com

Sustainable Development Goals, in particular, Goal 12: "Ensure sustainable consumption and production patterns".

Within this framework, cellulose has recently been used as a support of bioactive antibacterial compounds. In particular, quaternary ammonium salts as several bromide derivatives (DDTMABr, TDTMABr, HDTBPBr, DDTPPBr) showed their effective antibacterial activity against *Staphylococcus aureus*, *Escherichia coli*, *Candida albicans*, and *Pseudomonas aeruginosa*.[10] However, quaternary ammonium salt functionalization often requires long, multi-step, and resource-demanding procedures, with the possibility of undesired byproduct formation.[11] Materials containing $-NH_2$ moieties have also demonstrated good antimicrobial reduction levels.[12,13] Additionally, metal nanoparticles decorating cellulose, such as the well-known silver (Ag) and zinc oxide (ZnO), acted as bioactive compounds against *Escherichia coli*, *Staphylococcus epidermidis*, *Klebsiella oxytoca*, *Salmonella*, *Shigella dysenteriae*, *Shigella boydii*, and *Staphylococcus aureus*.[14–19] Recently, some of us have described the excellent antibacterial properties of aminopropyl waste cellulose-derived materials.[20] In that work, waste cellulose first underwent an extraction process from soybean hulls, and then a functionalization step was carried out to introduce aminopropyl groups. The optimization of the functionalization conditions was addressed by tuning the molar ratio of reagents, the solvent and the operating temperature. The more toxic toluene initially used as a solvent was successfully substituted by the more compatible ethanol, decreasing the synthesis temperature. That study was considered a starting point for developing cellulose-based materials that can be employed as antibacterial surfaces, textiles and filters for water depuration treatments. Despite this, some critical issues for sustainable production of these materials needed to be addressed. In fact, the synthetic procedure involved the use of organic solvents at their reflux temperature, implying non-negligible production costs (energy and raw materials).

In the current study, in view of the functionalization procedure optimization, water was used as a substitute for ethanol as an even greener solvent, and microwave (MW) irradiation was proposed as an alternative energy source to conventional thermal heating. Indeed, microwave-assisted methodologies are recently being applied to synthesize materials as low-energy impact procedures.[21,22] MW irradiation is rapid and allows homogeneous heating of the reaction mixture, with the advantages of high penetration, high speed, good radiation uniformity and low thermal inertia.[23,24] In particular, in the presence of lignocellulosic matter, it has been reported that the heating mechanism of microwave treatment involves dipole rotation and ionic conduction: lignocellulose-based materials absorb microwave energy due to the interaction between the polar molecules and the microwave electromagnetic field.[24]

Another issue presented in the previous study[20] was the elaborate procedure requested for cellulose isolation, consisting of the preliminary extraction of peroxidase followed by acid/basic treatments. With the scope of developing a sustainable production process, in terms of energy, raw materials and costs, bamboo powder without pretreatments has been used herein as the substrate for the functionalization of aminopropyl groups. Bamboo was chosen since it possesses a more complex composition (i.e., richer in lignin and hemicellulose than pristine soybean hulls), serving as a more representative material for a more com-

prehensive range of available lignocellulose-based biomass types. Bamboo -considered a giant grass- is widely studied in the literature as a sustainable, biodegradable and abundant material that is employable in different sectors, such as in the construction field, energy production, environmental remediation and food and biotechnology industries.[25–28] Exploiting bamboo as a lignocellulosic resource is also advantageous because of its inexpensive cost, fast-growing and role in CO_2 sequestration (carbon negative strategy).[29,30] Moreover, such biomass is disseminated worldwide, mainly in tropical and subtropical countries where water sanitization and antibacterial treatment are important topics that have a high social impact on poor communities. More in detail, bamboo is a lignocellulosic source material with various chemical and bio-macromolecular compositions depending on the species and genera. On average, the composition varied for holocellulose 45–85% (cellulose and hemicellulose), lignin 17–32%, total extractives contents 2–13%, and ashes content 1–6%.[31] The bamboo-based lignocellulose biomass's excellent mechanical and physical properties rely on the crystalline cellulose contents, hierarchical structure, and highly oriented 3D vascular bundles,[32] making bamboo a suitable natural resource for developing new hybrid materials and related microfluidic devices with catalytic and bioactive properties.[33–36] Regarding decontamination applications, for the first time in 2015, Kuan et al. prototyped a bamboo-based analytic platform to create a cheap and user-friendly point-of-care (POC) for chemical and bacterial detection in drinking water.[37] Successively, surface deposition of copper-based metal-organic framework (MOF199) was conducted on bamboo timbers to add new water-proof properties and antibacterial activities against *E. coli* and *S. aureus*.[38] Li et al. immobilized silver nanoparticles (Ag-NPs) into the bamboo vascular bundle for environmental applications in Chinese river and lake water remediation.[39] In the form of powder, bamboo was functionalized with chitosan and zinc oxide to confer antibacterial properties.[40,41]

In this work, a MW-assisted amino-functionalization procedure has been carried out on waste soybean hull-derived cellulose (as a reference) and bamboo powders using a water solution as a reaction medium. The so-prepared samples were compared with the corresponding samples synthesized by conventional thermal processes. All the materials were characterized in-depth. In order to verify the degree of functionalization, elemental analysis, thermogravimetric analysis and infrared spectroscopy were carried out. Differential scanning calorimetry was used in addition to thermogravimetry to investigate the thermal behavior of the materials. The structural and surface composition of the materials were addressed by X-ray diffraction and X-ray photoelectron spectroscopy, respectively. The morphology of the material was investigated by scanning electron microscopy. Finally, to understand how the synthetic approaches used could influence bioactivity, antibacterial tests on both Gram-positive and Gram-negative microorganisms were performed. Moreover, thinking of a possible application for scaling up the system for wastewater treatments,[42] the most promising materials were selected for simulating filters for water depuration and, thus, subjected to antibacterial tests under continuous flow.

Summarizing the various aspects taken into account so far, the key points related to the (ligno)cellulose amino-functionalization procedures that were adopted in this research are associated with

**ADVANCED
SCIENCE NEWS**

www.advancedsciencenews.com

**ADVANCED
SUSTAINABLE
SYSTEMS**

www.advsustainsys.com

the use of i) water as a unique solvent, ii) microwave as an alternative energy source, and iii) bamboo as a biomass exploited in its raw form. Moreover, the potentiality of the prepared hybrid materials to fight bacteria in water without the aid of nanoparticles or traditional antimicrobial substances (antibiotics, chlorine, etc.) represents another big advantage.

2. Experimental Section

2.1. Biomass Powder Types and Functionalization Procedure

The isolation of cellulose from soybean (*Glycine max*) hulls has been detailed previously: the product obtained after protein extraction and acid/basic hydrolysis resulted in a sufficient degree of cellulose cleanness after the removal of the other major hull components (hemicellulose and lignin).[20] Bamboo powder, instead, was obtained from a 4-year-old bamboo *Dendrocalamus giganteus Munro* collected from the botanic garden at PUC-Rio, Brazil, whose complete characterization can be found in recent papers.[34,35] In terms of composition, the bamboo powder herein employed showed the presence of cellulose, hemicellulose and lignin at 22%, 30% and 16%, respectively, plus some ashes and other minor components.

In a classical synthesis procedure inspired by the previous work,[20] a mixture of soybean hull-derived waste cellulose (W) or bamboo (B) powder (1 g) and 1.5 mL of (3-aminopropyl)triethoxysilane (APTES, 95%, Sigma-Aldrich) was refluxed in distilled water (20 mL) at 80 °C overnight. The material was filtered in vacuo and dried for 2 h at 100 °C. The prepared materials were labeled W1 and B1 for waste cellulose and bamboo precursors, respectively. Alternatively, APTES (1.5 mL) was added to a mixture of soybean-derived cellulose or bamboo powder (1 g) in water (20 mL) and the mixture was placed inside a conventional household microwave set at a power of 180 W, operating for 20 cycles (20 s on, 10 s off) with a total irradiation time of 6.40 min. The obtained products, labelled W_MW and B_MW, were filtered in vacuo and dried for 2 h at 100 °C. When necessary, further comparison with commercial cellulose as a reference was reported (Cellulose Fibers, medium, Sigma Aldrich).

2.2. Compositional and Physical-Chemical Characterization

Elemental analysis (C, H, N, S) was performed on pristine supports (B and W) and all the functionalized samples with a Thermo Nicolet FlashEA 1112 Series (Waltham, MA, USA) instrument. One of the main parameters considered was the Nitrogen content (% wt), as an indicator of NH_2-functionalization. The stability of functionalization was verified by washing the powders in deionized water two consecutive times (with each step of soaking and stirring lasting 3 h). After each period, a portion of the solid was separated and dried to be subjected to elemental analysis and to quantify the residual N amount with respect to the initial N value of non-washed samples.

The X-ray photoelectron spectroscopy (XPS) was conducted using a VG Microtech ESCA 3000 Multilab (VG Scientific, Sussex, UK), equipped with a dual Mg/Al anode. Un-monochromatized Al Kα radiation at 1486.6 eV was utilized as the excitation source.

The binding energies were referred to C1s energy, arising from adventitious carbon, based on a previous calibration at 285.1 eV. Peak analysis was performed with the CasaXPS software (Version 2.3.18PR1.0).

Attenuated total reflectance Fourier transform infrared (ATR-FTIR) spectra were recorded with a Thermo Nicolet iZ10 spectrometer (Milan, Italy) equipped with a Smart Endurance (ZnSe crystal) in the range 4000–650 cm⁻¹ with 32 scans and 4 cm⁻¹ band resolution. Diffusion reflectance infrared Fourier transform spectroscopy (DRIFTS) (Vertex 70, Bruker Optics, Ettlingen, Germany) was employed in the 4000–400 cm⁻¹ range with 128 scans and 2 cm⁻¹ band resolution.

The morphology of samples was investigated by using an EVO10 Scanning Electron Microscope (Carl Zeiss Microscopy GmbH, Germany) with an acceleration voltage of 20 kV. The samples were coated with a sputtered 20 nm-thick layer of gold through a Quorum Q150R ES Plus Sputter Coater (chamber conditions: 20 Pa of rarefied argon).

X-ray diffraction (XRD) analyses were performed using X-ray diffraction (XRD) measurements on a Bruker-Siemens D5000 X-ray powder diffractometer (Bruker AXS, Karlsruhe, Germany) equipped with a Kristalloflex 760 X-ray generator and a curved graphite monochromator using Cu Kα radiation (40 kV/30 mA) in reflection mode (Bragg-Brentano geometry). A proportional counter and 0.05° step sizes in 2θ were used. The assignment of the crystalline phases was based on the ICSD powder diffraction file cards (PDF 00-056-1718). In order to evaluate differences in crystallinity among the different samples, the crystallinity index CI (%) was calculated through the tools in OriginPro 2023 software. The peaks due to crystalline cellulose and amorphous cellulose were added to perform deconvolution (Gaussian functions). Then, the CI (%) was determined according to the following equation (Equation 1):[43,44]

$$CI\ (\%) = \frac{Sc}{St} \times 100 \tag{1}$$

where Sc represents the area of the crystalline domain and St the area of the domain in the range 10–30 ° 2θ, respectively.

Segal and co-workers[45] developed another method for finding the CI (%), taking into account only one reflection of cellulose I lattice (200), which appears at around 2θ = 22.5°. In this method, crystallinity was calculated by comparing the (200) peak intensity to that at the minimum between the (200) and (110) peaks (the height is measured approximately at 18 °).

The average crystallite size was calculated by means of Scherrer's equation (Equation 2) applied on the (200) peak (typical of cellulose diffractograms).

$$d = \frac{K\lambda}{\beta \cos\theta} \tag{2}$$

where d = coherent diffraction domain size, λ = the wavelength of the X-ray source applied, β = the reflection width (2θ), θ = the Bragg angle and K = the shape constant.

The thermal characteristics of the samples were studied by thermogravimetric analysis (TGA) and differential scanning calorimetry (DSC). TGA analyses (TGA 1 Star System of Mettler Toledo, Schwerzenbach, Switzerland) were conducted on about 10 mg of sample that was brought from room temperature to

**ADVANCED
SCIENCE NEWS**

www.advancedsciencenews.com

**ADVANCED
SUSTAINABLE
SYSTEMS**

www.advsustainsys.com

100 °C, left at this temperature for 30 min and then heated to 1000 °C at a rate of 10 °C min^{-1} in 30 mL min^{-1} of nitrogen flux. Derivative thermogravimetry (DTG) was employed to identify the temperature of maximum mass-loss rates. Differential scanning calorimetry (DSC) was carried out with a DSC calorimeter (Mettler Toledo 821e, Schwerzenbach, Switzerland) calibrated by an indium standard. The DSC cell was flushed with N_2 at 100 ml min^{-1}. The run was performed in the temperature range 30–500 °C, at the heating rate of 10 °C min^{-1} and the mass sample was about 5 mg. STARe Software was used to process the resulting data.

2.3. Antibacterial Tests

The antibacterial activity of the biomass-based samples was tested following the ASTM E 2149-2013 procedure "Standard test method for determining the antimicrobial activity of immobilized antimicrobial agents under dynamic contact conditions." The bacteria were *Escherichia coli* ATCC 11229 (Gram-negative) and *Staphylococcus aureus* ATCC 6538 (Gram-positive).

The bacteria were grown in a nutrient broth (Buffered peptone water for microbiology, VWR Chemicals) for 24 h at 37 °C. The bacteria concentration was measured with a spectrophotometer and diluted into a sterile buffer to give a 1.5–3.0×10^5 CFU mL^{-1} working dilution. This bacterial inoculum was put in contact with the antibacterial agent (cellulose/bamboo powder) under shaking at room temperature for 1 h using the standard antibacterial powder:inoculum ratio of 1 g:50 mL. After this time, 1 mL of inoculum was diluted 1000 times and plated in Petri dishes with yeast extract agar (Sigma Aldrich). The Petri dishes were incubated at 37 °C for 24 h and subsequently, the surviving bacteria colonies were manually counted and compared to the initial bacteria concentration of the inoculum to calculate the % bacterial reduction using this equation (Equation 3).

$$\text{Reduction} \ (\%) = \frac{(A - B) \times 100}{A} \quad (3)$$

where: A = number of viable microorganisms before treatment, B = number of viable microorganisms after treatment. The standard deviation of the antibacterial tests calculated on three replicates has been determined <10%.

W1 and B1 were also tested in different conditions, namely a continuous mode, letting the inoculum of *Escherichia coli* continuously flow through the antibacterial samples. The setup was composed of a peristaltic pump (Millipore), Tygon tubing (Merck, Germany) and a sterilized plastic filter holder (25 mm internal diameter, Sartorius Stedim Biotech GmbH, Germany). W1 and B1 powders were uniformly distributed between two disks (25 mm) of filter paper Whatman Grade 1 (Sigma Aldrich, particle retention of 11 μm). The sandwich containing the antibacterial sample (200 mg for W1 and 80 mg for B1) was placed in the filter holder. The explanation of the different amounts of powder used for W1 and B1 is reported in the Results and Discussion section. After setting the filter holder loaded with antibacterial agents at the extremity of the pump equipment, 20 mL of the *E. coli* bacterial inoculum, prepared following the same ASTM E 2149-2013 procedure, was pumped from the reservoir at 5.4 mL min^{-1} flow rate in the system. Approximately every 3 min, 1 mL
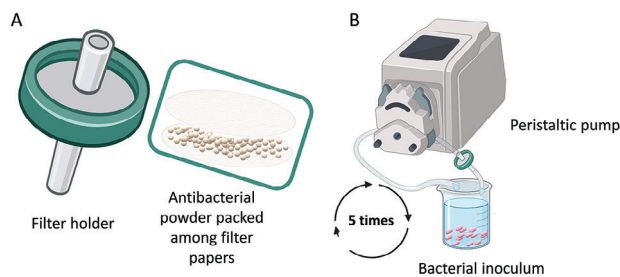

Figure 1. Representation of antibacterial tests conducted in a continuous flow, where A) shows the preparation of the active filter and B) the overall setup.

of inoculum was taken from the reservoir and pleated in yeast extract agar. The inoculum was cycled in the system, letting the entire volume of bacterial inoculum (diminished over time of the withdrawn aliquots) pass through the filter five times for a total of ca. 17 min. For the sake of clarity, the trial setup is reported in **Figure 1**.

3. Results and Discussion

3.1. Composition and Stability

The functionalization of the bamboo and cellulose has been confirmed by XPS, thanks to the presence of the peaks at 103 and 399.5 eV due to Si2p and N1s photoemissions.[46] N1s binding energy values are typical of the amino group. The lower N/C ratio (see **Table 1**) than Si/C might indicate the leaching of some lateral NH_2-containing moieties during the grafting process or the reversed or folded configuration of APTES molecules, causing the XPS nitrogen signal attenuation by the limited electron mean free path.[47–49] Comparing N/C ratios from XPS (more related to surface composition) with those obtained from CHNS (Table 1), in the case of W1 and W_MW, it is possible to see that the two values are coherent (starting W-cellulose does not contain N). Contrarily, bamboo-derived samples intrinsically contain nitrogen also in bulk (reference bamboo N/C = 0.006) and B_MW achieved a lower functionalization degree than B1.[50]

Regarding stability, the lowest total leaching values after two washing cycles were observed for the samples prepared with

Table 1. Chemical composition data from XPS and CHNS analyses and Nitrogen leaching degrees after two washing cycles.

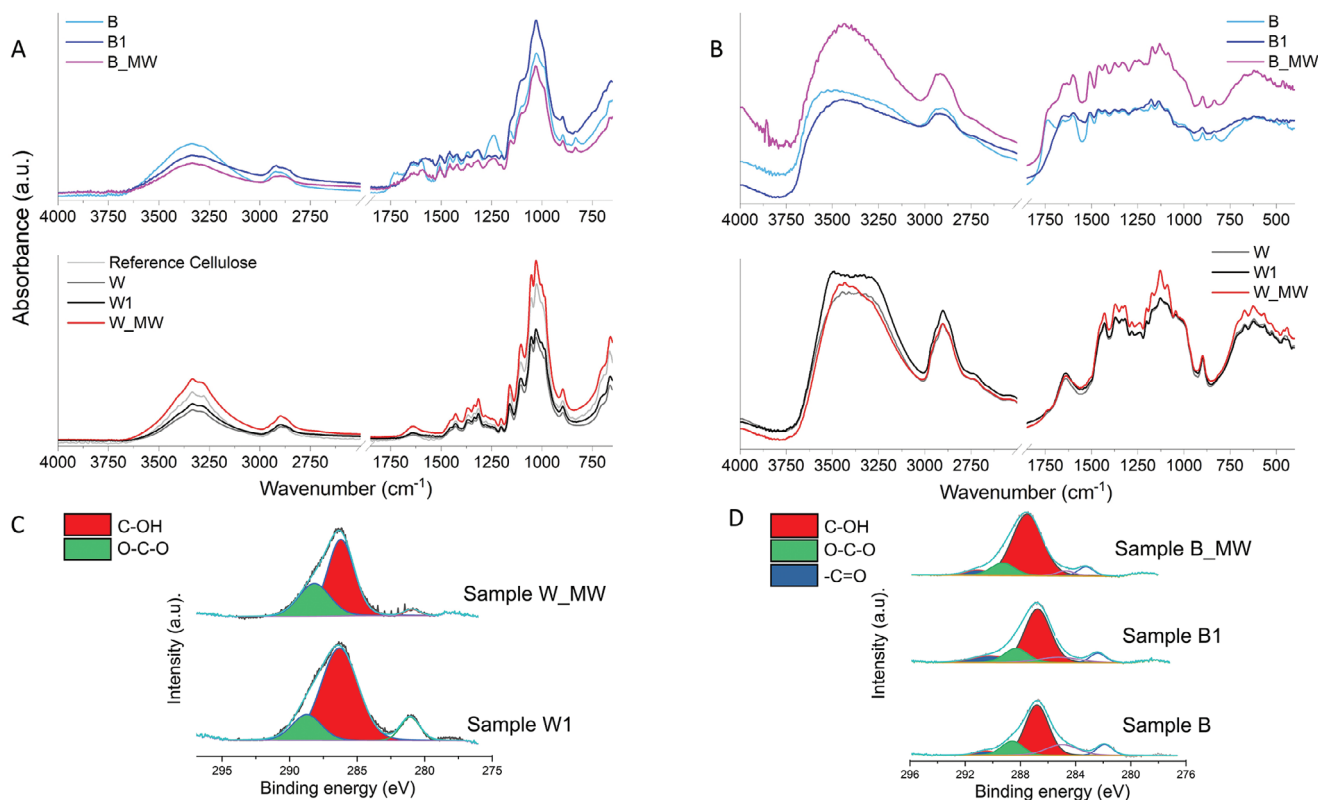| Sample	N/C (CHNS)	N/C (XPS)	Si/C (XPS)	C1s	Total N leaching
W1	0.01	0.01	0.07	286.3 (82%) 288.8 (18%)	38%
W_MW	0.01	0.01	0.09	286.2 (66%) 288.5 (34%)	48%
B1	0.04	0.02	0.10	286.7 (71%) 288.3 (17%) 290.2 (12%)	24%
B_MW	0.02	0.01	0.08	286.5 (81%) 288.3 (13%) 290.2 (6%)	43%

Figure 2. Spectra recorded in A) ATR-FTIR, B) DRIFT modes; C1s region of materials from XPS for C) W-series and D) B-series. In (A), reference cellulose indicates the commercial fibrous cellulose sample.

the conventional thermal procedure. It has to be underlined that, after the first washing step, the release continued to the greatest extent in the presence of B_MW (21%), whereas the other specimen leaching was limited to a maximum of 14% (bare bamboo has also been subjected to the release of the inherently present nitrogen). It has been previously assumed that the APTES molecules most prone to be desorbed are the monomeric species, whereas a firmer anchoring has been attributed to self-condensed silanes.[46,51] Moreover, the lower efficiency of MW-assisted synthesis can be attributed to the low temperature reached in the adopted conditions, <80 °C.[52–54]

ATR-FTIR of W- and B-derived samples are illustrated in **Figure 2A**. For W-series, the main signals, typical of cellulose,[20] are: i) the band in the wavenumber range of 3400–3200 cm^{-1} (assignable to O—H and, when present, N—H stretching), ii) the peaks at 2970 and 2840 cm^{-1} (related to —CH$_2$ asymmetric and symmetric stretching vibrations), and iii) the prominent band in the spectrum region 1200–950 cm^{-1} (attributable to C—O, C—O—C of pyranose ring skeleton and C—OH groups). The peak positioned at about 1630 cm^{-1} is due to adsorbed water, whereas between 1450 and 1230 cm^{-1}, there are the characteristic signals of other —CH$_2$ and C—H deformations. At ca. 900 cm^{-1}, the β-glycosidic linkage signal appears.[55] For the functionalized samples, the small shoulder around 1560 cm^{-1} has been assigned to the N—H bending of primary amines[20] and it is consistent with APTES attachment. The bamboo absorptions are more complex and, regarding the spectral regions already analyzed for W-celluloses, presented these differences: i)

a smoother band in the —OH/—NH region at high wavenumbers (due to different hydrogen bondings, i.e., given by phenolic portions[56]), ii) broader peaks related to methyl and methylene groups (3000–2750 cm^{-1}) and carbohydrate region (1250-950 cm^{-1}). From 1800 to 1200 cm^{-1}, the bamboo powder sample showed its peculiar series of signals that, according to previous works,[57,58] are non-conjugated carbonyl stretching at 1730 cm^{-1}, conjugated carbonyl stretching at 1640 cm^{-1} and aromatic skeletal vibration at 1600, 1505 and 1460 cm^{-1}, typical of lignin and hemicellulose. It is possible to observe a reasonable indication of the grafting occurrence in correspondence to the disappearance of the peak at 1736 cm^{-1} for B1 and B_MW. This fact allowed us to hypothesize that C=O groups are further points of attack, other than cellulosic hydroxyls, during the bamboo reaction with APTES.

DRIFT spectra were also recorded to search for other particular discrepancies among the samples (Figure 2B), since such a spectroscopical technique, often applied to powders, implies a diffusely scattered light derived from multiple reflections of incident radiation within the sample.[59] In general, the absorption positions of both ATR and DRIFT correspond to the same functional groups.[60] The peculiar points that can be first noticed in DRIFT spectra of the W-series regard the region at high wavenumbers. The sample W_MW has a sharp peak at 3433 cm^{-1}, with respect to the "flatter" and doubled band of W and W1. Such signal modification can represent the transformation of the hydrogen bonding network, and it can be associated with an increase in crystallinity, which goes hand in hand with the intensity
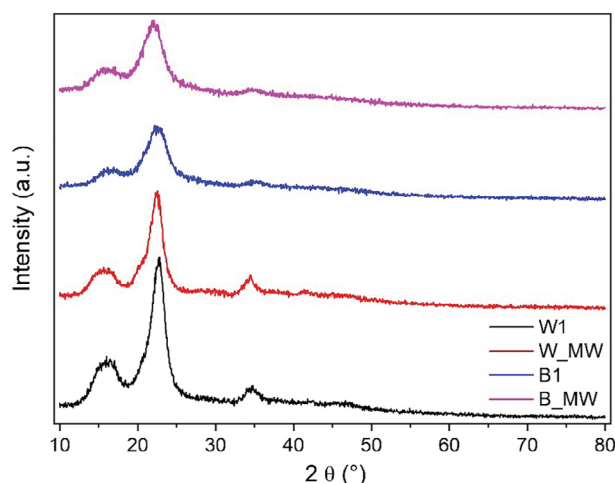
ADVANCED
SCIENCE NEWS

www.advancedsciencenews.com

ADVANCED
SUSTAINABLE
SYSTEMS

www.advsustainsys.com

Figure 3. X-ray diffraction patterns for W1, W_MW, B1 and B_MW.

enhancement of the vibrations at 1430 cm^{-1} and 1370 cm^{-1}.[61,62] In the case of bamboo-derived samples, the main peak at 3440 cm^{-1} for B1 and B_MW was shifted compared to the bare bamboo powder, again suggesting modifications to the hydrogen bonding network after amino-functionalization. Regarding the evaluation of grafting procedure success, the carbonyl peak at 1737 cm^{-1} completely disappears in B1, whereas it remains as a shoulder in B_MW, confirming ATR results and the hypothesis of APTES interaction with carbonyl groups. Furthermore, around 1560 cm^{-1}, the bare bamboo spectrum has a valley that changes its rounded shape in functionalized samples, probably due to the amino group presence.

In order to investigate the functional groups more deeply, the C1s regions acquired by XPS for different powders are displayed in Figure 2C,D. Both W- and B-materials showed the main peaks at ca. 287 eV, typical of the C—OH bond, and at ca. 288 eV, ascribable to O—C—O bonding[46] (see Table 1 for percentage values). Additionally, bamboo-derived samples possessed the peak related to —C=O (290 eV).[63]

3.2. Microstructural, Thermal, and Morphological Characterization

XRD patterns of samples resemble crystalline cellulose type Iβ, with the main peaks at 14.5°, 16.5°, 20.5° and 22.5° 2θ attributed to the planes (1 -1 0), (1 1 0), (1 0 2) and (2 0 0) respectively, and an amorphous component (**Figure 3**).

Through the deconvolution method, the CI (%) for W1 was 61% and, for W_MW, it was 69%. The CI (%) obtained with the Segal estimation was higher, >85% (as often occurs with this method[44]). For B1 and B_MW, as reasonable, the amount of non-crystalline components was more significant[57,64] and the microwave effect seemed inverted: B_MW reached a CI (%) value of 43%, whereas for B1 it was 48% (a trend also confirmed using the Segal method). Some considerations concerning the lack of a trend could be made, ascribing it to a different interaction of the two biomasses towards microwaves. In general, it has been reported that, in the presence of oxygen-containing species like cellulose, microwaves can influence the C—O bond

length at lower power and hydroxyl groups at higher power.[65] Sadeghi-Shapourabadi et al.,[66] who studied nano-fibrillated cellulose from potato peel waste, assumed that microwaves, in addition to the elimination of non-crystalline components, can induce the hydroxyl groups of cellulosic chains to form intramolecular and intermolecular hydrogen bonds. Such bonding hinders the free cellulose chain movements, favoring the creation of an orientation and, therefore, increasing the crystallinity values. This phenomenon has also been reported for bamboo-based materials,[67] but what we observed in this work can be more related to the modification of the complex matrix of bamboo formed by different components[68] and the type of cellulose chain arrangement. Indeed, Wang et al. noticed that the structure of bamboo cellulose was altered by microwave treatment, resulting in the transformation of cellulose from the crystalline region to para-crystalline,[69] where paracrystalline cellulose has been defined as a non-equilibrium intermediate structure between amorphous and crystalline states.[70] Furthermore, crystallite sizes for W-derived samples were estimated at about 4.5 nm and for B-series ca. 3 nm, which are in good agreement with the literature.[57,71–73]

Thermal analyses were carried out by both TGA and DSC techniques (**Figure 4**).

It is possible to notice that W1 and W_MW TGAs were almost superimposable before 400 °C and started their degradation at higher temperatures than other samples. The phenomena visible in the DTG occurring between 250–300 °C, especially in bamboo-derived samples, can be attributed to the presence of other biomass components, especially hemicellulose.[74,75] The final weight loss percentages were: 87% for W-cellulose, 85% for W1, 83% for W_MW, 77% for bamboo powder B, 62% for B1 and 71% for B_MW. The differences between these values correlate to the silicon-based functionalization moieties and to the presence of the non-cellulosic portion, which caused the formation of char and ashes in a nitrogen atmosphere, increasing the residue at 1000 °C.[76,77]

Regarding DSC outcomes, all the main heat exchange events correlated to carbohydrates and lignin were centered in the 354–364 °C range. From the inspection of the shapes of the calorimetric curves, the peaks of W1 and W_MW are well-defined as typical cellulose powders, even sharper than the original W sample. The enthalpy obtained from the area integration of W1 peak at 363 °C was higher than W_MW (278 vs 204 J g^{-1}), and the water evaporation-related peak within 150 °C was more pronounced for W_MW (the accessibility to water has been related to the amorphous fraction[78]). This double evidence may lead to hypothesizing a lower crystallinity for W_MW, in contrast to the above-presented XRD and DRIFT elaborations.

The thermal-induced phenomena in the presence of bamboo-derived samples are less intense than in the W-samples and distributed along a wider range of temperatures since they underlie the heat exchanged by different bamboo components. In the case of B1, a significant event related to water evaporation (centered at ca. 80 °C) took place, and exothermic peaks were recorded after 250 °C, differently from the other specimens. These two observations can be related, respectively, to the greater presence of amorphous regions[78] and to the predominance of the depolymerization reactions at the expense of amorphous parts, also influenced by the highest presence of APTES[79,80] (see Table 1). Again, these
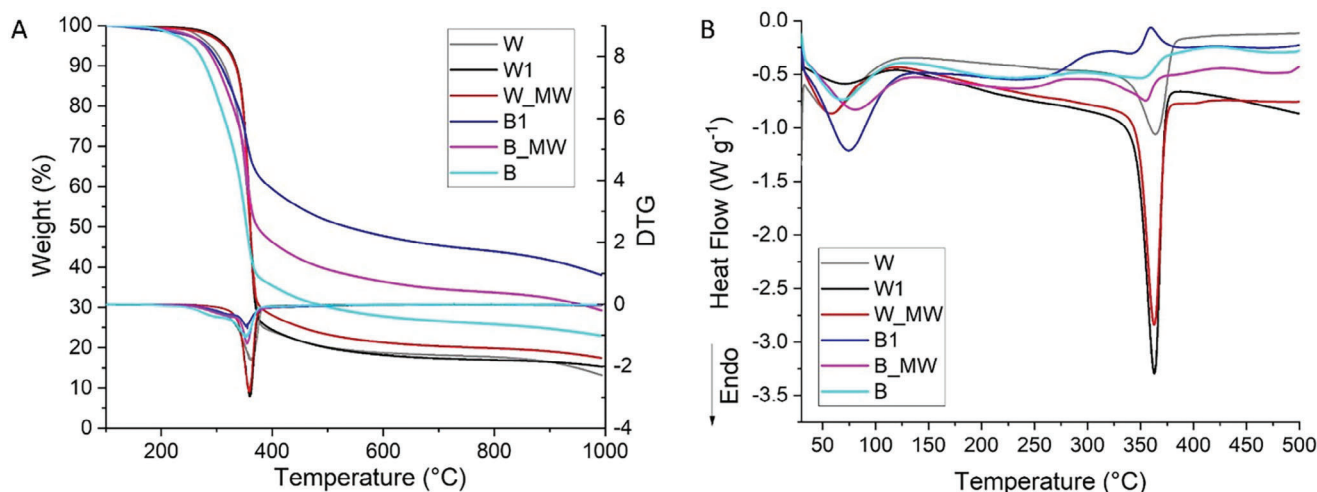
ADVANCED
SCIENCE NEWS

www.advancedsciencenews.com

ADVANCED
SUSTAINABLE
SYSTEMS

www.advsustainsys.com

Figure 4. A) TGA and DTG profiles. B) DSC results.

results apparently contradict the XRD CI(%) determination if we compare B1 and B_MW behaviors.

Although the discrepancies emerging from XRD and DSC results do not allow the formulation of a solid hypothesis regarding the effect of microwaves on the crystalline structures of the examined biomasses, they give the opportunity to discuss the reasons for these outcomes. The two techniques exploit completely different physical-chemical mechanisms and are obviously conducted in different conditions, one among all, in terms of operating temperatures. Going into detail, DSC phenomena for cellulose-based samples involve an overall thermal degradation, not only at the expense of the crystalline fraction. A critical point arising from XRD evaluation, instead, is the presence of small crystallites, which are plausibly incorporated into the amorphous contribution through the common fitting procedures,[72,81] potentially causing misinterpretations. Moreover, in the case of XRD, the original dataset must undergo manipulation (graphic elaboration, peak fitting, etc.).

The issues related to a nonunivocal crystallinity determination-firstly, the lack of absolute crystalline and amorphous standards-

have already been expressed in a recent paper by Salem et al.,[81] who compared XRD-based methods with Nuclear Magnetic Resonance, Raman, Infrared and Sum-Frequency Generation spectroscopies.

From SEM analyses in **Figure 5**, the fibers of soybean-derived cellulose samples (W, W1 and W_MW), with median length distribution centered between 30 and 40 µm and width of 5–10 µm, did not show morphological differences in dependence on the functionalization treatment. The cemented regions were already detected in the previous paper and ascribed to residual soybean hulls' matrix components.[20,82] Bamboo-derived samples (B, B1 and B_MW) are characterized by the presence of bundles of fibers with lengths in the order of magnitude of some hundreds of micrometers and diameters for single fibers of about 15–30 µm. Areas of "disordered" and non-fibrous matter have also been detected (see, for instance, the bottom part of the image related to sample B), as well as metaxylem vessels with reticulate and pitted thickenings (see the central area of the figure with sample B1).[32,83] Although parenchymal cells are typical of the structure and, thus, of the morphology of bamboo, they have been revealed
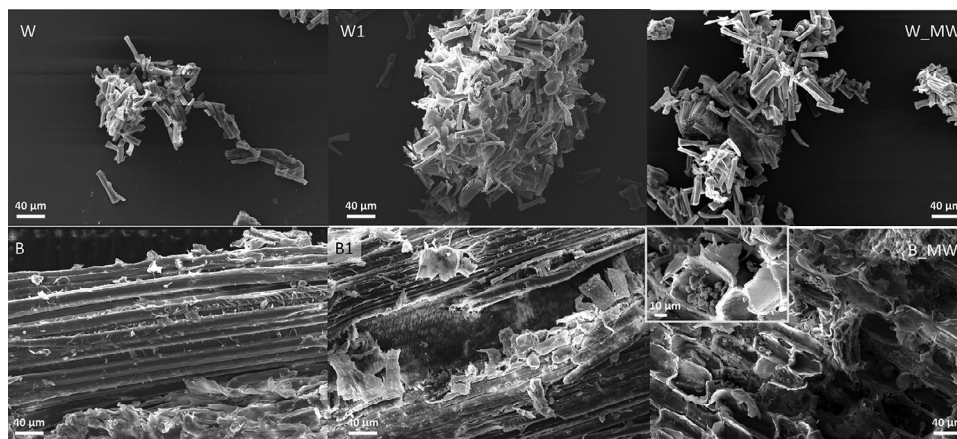

Figure 5. SEM images of various samples at the same magnification (scale bar = 40 µm); in the inset of the sample B_MW, a micrograph at higher magnification of the sample has been reported.

Table 2. Reduction of *Escherichia coli* and *Staphylococcus aureus*, operated by different samples under study, following the ASTM E 2149-2013 procedure.

Sample	Bacterial reduction [%]	
	E. coli	*S. aureus*
Reference cellulose[a]	15	0
W[a]	52	0
B	0	0
W1	100	99.5
W_MW	100	99.5
B1	100	98.6
B_MW	100	93.8

[a] Reference cellulose and W values are taken from.[20]

by this SEM exploration only in the case of B_MW, probably because the microwave treatment caused a certain separation from other matrix components[84,85] and a higher exposition of these tissues. Starch granules in the parenchyma cells are presented in the micrograph inset of sample B_MW.[86]

3.3. Antibacterial Activity

Data in **Table 2** summarize the antibacterial efficiencies of all the materials examined. Reference cellulose and W values come from,[20] and it is worth briefly recalling that the activity of bare W cellulose against *E. coli* was attributed to residual polyphenolic substances, typical of soybean hull composition and eventually freed/exposed after the isolation procedure. Contrarily, the bamboo powder alone did not demonstrate any activity toward both strains. This result is interesting since the real effectiveness of bamboo fibers' non-extracted polyphenols in removing or resisting microorganisms is debated in the literature.[87–89] Polyphenols are, indeed, well-known antioxidant and antimicrobial substances exploiting hydroxyl groups' action.[90] Their antimicrobial activity principally occurs by destroying microorganism cells and, subsequently, inhibiting intracellular functions.[91]

Table 2 also shows that, in general, the functionalized biomass samples reached an excellent degree of bacterial removal. The mechanism that rules such activity must be searched in the function of amino groups as cationic sites, therefore following a recognized pathway: i) adsorption and penetration into the negatively-charged bacterial cell wall; ii) reaction with the cytoplasmic membrane (lipid or protein) leading to membrane destabilization; iii) release of intracellular low-molecular-weight substances; iv) degradation of proteins and nucleic acids; and v) wall lysis caused by autolytic enzymes.[92,93] Nevertheless, the presented results also reveal that the removal of *E. coli* was complete for all the materials under examination, while for *S. aureus*, a minimal bioactivity decrement was observed. This slight difference is ascribable to the diverse bacterial cell membrane compositions of Gram-positive and Gram-negative strains. Indeed, Gram-negative bacteria cell walls are composed of thin peptidoglycan layers, surrounded by an outer membrane containing lipopolysaccharides, whereas Gram-positive bacteria are devoid of an outer membrane

but are surrounded by thicker layers of peptidoglycans.[94] These characteristics can lead to different microorganism's susceptibilities to antimicrobial agents.

All considered, the grafting procedure applied in this work was confirmed as a valuable method to obtain strong antibacterial materials. This statement can also be sustained by taking into account previous attempts:[20] all the chosen synthesis conditions, namely changing the solvent and the biomass types and using microwaves, still led to highly efficient materials. On an earlier occasion,[20] the performances of our aminated celluloses were compared to other cationic celluloses (functionalized with quinolinium[95] or phenanthridinium[96] silane salts and peptides[97]), standing out for their optimal activity against Gram-negative and positive strains, even in exiguous quantities. Further validation of the interesting performances of our materials can be found by deepening the most recent literature scenario. Carvalho et al.[98] pointed out that suspensions of amino-modified cellulose nanocrystals (prepared by tosylation and subsequent reaction with ethylenediamine) showed a limited bactericidal effect against *S. epidermidis* and *E. coli*. Serizawa et al.[99] enzymatically amino-functionalized nanocellulose and further added ethylenediaminetetraacetic acid (EDTA), obtaining materials capable of destabilizing the cell wall of *E. coli* but not of *S. aureus*. Regarding the functionalized bamboo, chlorocholine chloride/urea (ClChCl-urea) was used by Ye et al.[100] as a deep eutectic solvent to achieve cationized bamboo fibers. The solvent of ClChCl-urea partially removed the bamboo non-cellulosic substances and the obtained material exhibited bacteriostatic rates of 75.5% and 72.7% toward *E. coli* and *S. aureus*, respectively. Szadkowski et al.,[101] instead, prepared hybrids of APTES onto bamboo fibers (using toluene as the reaction solvent) and did not notice any antibacterial activity against *E. coli*, *S. aureus*, and *B. subtilis*.

In order to make a step forward in our research, cellulose and bamboo-derived samples prepared through the thermal method, namely W1 and B1, were selected as the best materials in terms of performance and stability to be adopted in antibacterial experiments conducted under continuous flow. They have been used in different amounts, given the different physical packing capacities of the powders, to avoid leaching from the sample holder. W1 amount was 200 mg, whereas the employed B1 mass was 80 mg. Moreover, the two powders have slightly different bulk densities (comprised between 0.22 and 0.26 g cm^{-3}, not far from the literature results[102–104]). Considering these premises and the fact that the contact time was proportional to the void volume of the powder sandwiched between paper filters, the contact between the solution containing bacteria and B1 was more prolonged than in the case of W1. Although this factor, W1 kinetics of bacterial reduction was faster, indicating that the concentration of antibacterial agent was fundamental in the first moments of this process (see **Figure 6**). However, after only 17 minutes, *E. coli* removal action was complete for both materials, corroborating their outstanding performances and their applicability in filters for water decontamination. According to the studies reported in,[20] indeed, antibacterial tests performed by both reducing the functionalized powder amount up to 10000 folds or by reusing materials that partially lost nitrogen showed that the decontamination ability of the NH$_2$-grafted cellulose-based materials could be retained even in more severe conditions.
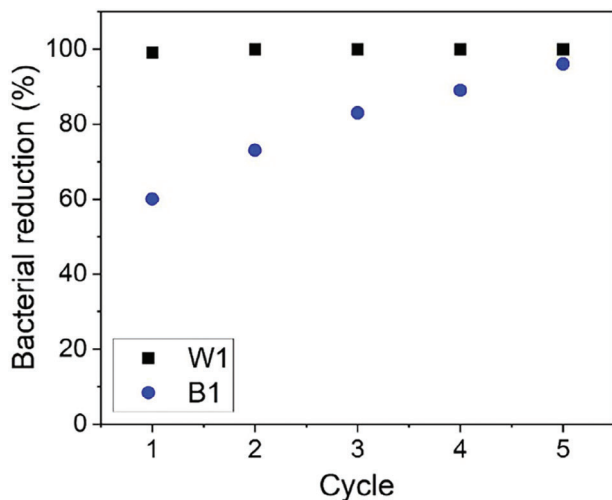
Figure 6. Five-cycle continuous flow tests of W1 and B1 against *Escherichia coli*.

Certainly, the partial nitrogen loss makes the activity of these materials attributable, at longer times, to both heterogeneous and homogeneous phenomena, needing further optimization studies. However, imagining a possible impact of APTES release, it has been found that this reactant is relatively safe in terms of cytotoxicity.[12,77,105]

4. Conclusions and Perspectives

In this work, starting from pre-existent knowledge, soybean hull-derived cellulose and non-pretreated bamboo powders were functionalized with APTES (bearing aminopropyl groups) to impart antibacterial properties and evaluate the impact of different kinds of biomass as substrates. Moreover, with respect to previously adopted syntheses, the aminopropyl groups were grafted in water as a unique solvent, either following a thermal-based procedure (heating at 80 °C) or using microwaves as the energy source.

Despite the advantages in terms of time, energy, and cost demand associated with using microwave radiation instead of the conventional thermal route, the physical-chemical characterizations showed a higher instability of the samples prepared using the MW-assisted procedure (higher leaching of nitrogen). Indeed, this methodology needs condition adjustments and optimization to exploit all potentialities. Regarding the differences seen in correspondence with the use of diverse biomass substrates, it was possible to hypothesize that bamboo powder reacted with the grafting agents using functionalities other than hydroxyl groups (i.e., carbonyl), brought about by hemicellulose and lignin. Other differences related to the bamboo complex matrix were detected in thermally induced behavior (from TGA/DSC outputs) and morphology (from SEM investigation).

The antibacterial trials performed on Gram-negative and Gram-positive strains (*E. coli* and *S. aureus*, respectively) showed, in general, bacterial reductions comprised between 93% and 100%. The action mechanism of the prepared materials was elucidated and attributed to the ability of amino groups to destabilize bacterial cells. Moreover, moving forward to a possible applicative upscale, the tests carried out using the powders as filters for wa-

ter decontamination in a continuous flow demonstrated that the cellulose-based sample was able to reach a total bacterial reduction against *E. coli* in the first minutes, whereas functionalized bamboo required 17 min. The reasons could be related to the filter packing conditions that allowed a lower presence of bamboo-derived powder and, therefore, a lower availability of -NH$_2$ moieties.

To summarize, employing amino groups to functionalize different (ligno)cellulosic materials in even greener synthetic conditions has been revealed to be a convenient tool for developing novel and efficient antibacterial hybrids, as also evidenced by the comparisons with other studies. Efforts need to be made to increase the stability of such materials while maintaining mild synthesis conditions and to understand their biocompatibility for application in real waters. However, the strategies employed in this study, also thanks to previous investigation findings, can be further applied to the creation of other bioactive materials, such as antibacterial fabrics.

4.1. Ethics Approval and Consent to Participate

This article does not contain any studies with human participants or animals performed by any of the authors. The authors claim compliance with the ethical standards.

Conflict of Interest

The authors declare no conflict of interest.

Author Contributions

The study was mainly designed by M.L.T., O.G.P., and M.L.T. Material preparation was performed by M.L.T., E.L., and M.L.T.; data collection and analyses were conducted by M.L.T., O.G.P., C.C., V.L.P., C.V. The first draft of the manuscript was written by M.L.T., and all authors commented on and revised it. All authors read and approved the final manuscript.

Data Availability Statement

The data that support the findings of this study are available from the corresponding author upon reasonable request.

Keywords

amination, antibacterial activity, bamboo, biomass, soybean hulls

[1] M. L. Tummino, I. Cruz-Maya, A. Varesano, C. Vineis, V. Guarino, *Materials* **2024**, *17*, 2435.

[2] EUROPEAN FOOD SAFETY AUTHORITY, Antimicrobial resistance, https://www.efsa.europa.eu/en/topics/topic/antimicrobial-resistance (accessed: July 2024).

[3] A. L. Srivastav, N. Patel, V. K. Chaudhary, *Environ. Pollut.* **2020**, *267*, 115474.

[4] N. N. Solihat, A. F. Hidayat, R. A. Ilyas, S. M. K. Thiagamani, N. I. W. Azeele, F. P. Sari, M. Ismayati, M. I. Bakshi, Z. N. Garba, M. H. Hussin, W. K. Restu, W. Syafii, H. A. Ariyanta, W. Fatriasari, *J. Bioresour. Bioprod.* **2024**, *9*, 283.

[5] X. Dang, Y. Fu, X. Wang, *Adv. Funct. Mater.* **2024**, *34*, 2405745.

[6] F. Ali, A. Dawood, A. Hussain, M. H. Alnasir, M. A. Khan, T. M. Butt, N. K. Janjua, A. Hamid, *Discover Sustainability* **2024**, *5*, 156.

[7] X. Dang, N. Li, Z. Yu, X. Ji, M. Yang, X. Wang, *Carbohydr. Polym.* **2024**, *342*, 122385.

[8] M. Yadav, M. Agarwal, *Mater. Today Proc.* **2021**, *43*, 2895.

[9] W. Zhang, P. Zhang, H. Wang, H. Li, S. Y. Dai, *Trends Biotechnol.* **2022**, *40*, 1519.

[10] N. S. Nemeş, C. Ardean, C. M. Davidescu, A. Negrea, M. Ciopec, N. Duţeanu, P. Negrea, C. Paul, D. Duda-Seiman, D. Muntean, *Polymers* **2022**, *14*, 8.

[11] X. Fu, Y. Zhang, X. Jia, Y. Wang, T. Chen, *Molecules* **2022**, *27*, 1267.

[12] W. Shao, J. Wu, H. Liu, S. Ye, L. Jiang, X. Liu, *Carbohydr. Polym.* **2017**, *178*, 270.

[13] R. Koshani, J. E. Eiyegbenin, Y. Wang, T. G. M. van de Ven, *J. Colloid Interface Sci.* **2022**, *607*, 134.

[14] S. Pal, R. Nisi, M. Stoppa, A. Licciulli, *ACS Omega* **2017**, *2*, 3632.

[15] M. Onyszko, A. Markowska-Szczupak, R. Rakoczy, O. Paszkiewicz, J. Janusz, A. Gorgon-Kuza, K. Wenelska, E. Mijowska, *Sci. Rep.* **2022**, *12*, 1321.

[16] N. H. Nguyen, T. P. Le, T. B. N. Duong, V. K. Le, H. H. Do Ho, L. H. T. Nguyen, T. Le Hoang Doan, N. X. D. Mai, L. M. T. Nguyen, N. K. Pham, *Appl. Biochem. Biotechnol.* **2024**, https://doi.org/10.1007/s12010-024-04868-9.

[17] B. El Allaoui, H. Chakhtouna, A. Ouhssain, I. M. Kadmiri, H. Benzeid, N. Zari, A. el kacem Qaiss, R. Bouhfid, *Int. J. Biol. Macromol.* **2024**, *273*, 133078.

[18] A. Zeng, R. Yang, Y. Tong, W. Zhao, *Int. J. Biol. Macromol.* **2023**, *235*, 123739.

[19] M. S. Rana, M. A. Rabbi, M. F. Begum, S. M. Hoque, M. M. Rahman, M. A. Rahman, H. Ahmad, *Carbohydr. Polym. Technol. Appl.* **2024**, *8*, 100554.

[20] M. L. Tummino, E. Laurenti, P. Bracco, C. Cecone, V. La Parola, C. Vineis, M. L. Testa, *Cellulose* **2023**, *30*, 7805.

[21] J. Qu, Q. Meng, X. Lin, W. Han, Q. Jiang, L. Wang, Q. Hu, L. Zhang, Y. Zhang, *Sci. Total Environ.* **2021**, *752*, 141854.

[22] G. Gautier di Confiengo, M. G. Faga, V. La Parola, G. Magnacca, M. C. Paganini, M. L. Testa, *Mater. Chem. Phys.* **2024**, *321*, 129485.

[23] E. Vialkova, M. Obukhova, L. Belova, *Water* **2021**, *13*, 1784.

[24] J. Du, K.-L. Yang, Z.-Q. Yuan, Z.-M. Liu, X.-Y. Li, S.-J. Liu, C.-C. Li, S. Meng, R.-M. Wu, *Constr. Build. Mater.* **2023**, *394*, 132170.

[25] K. M. F. Hasan, K. N. Al Hasan, T. Ahmed, S.-T. György, M. N. Pervez, L. Bejó, B. Sándor, T. Alpár, *Case Stud. Chem. Environ. Eng.* **2023**, *8*, 100362.

[26] A. Emamverdian, Y. Ding, F. Ranaei, Z. Ahmad, *Sci. World J.* **2020**, *2020*, 7284203.

[27] L. Binfield, T. L. Britton, C. Dai, J. Innes, *Environ. Evidence* **2022**, *11*, 33.

[28] D. Kalderis, A. Seifi, T. Kieu Trang, T. Tsubota, I. Anastopoulos, I. Manariotis, I. Pashalidis, A. Khataee, *Environ. Res.* **2023**, *224*, 115533.

[29] J. Q. Yuen, T. Fung, A. D. Ziegler, *For. Ecol. Manage.* **2017**, *393*, 113.

[30] X. Xu, P. Xu, J. Zhu, H. Li, Z. Xiong, *Sci. Total Environ.* **2022**, *814*, 152697.

[31] F. Rusch, A. D. Wastowski, T. S. de Lira, K. C. C. S. R. Moreira, D. de Moraes Lúcio, *Biomass Convers. Biorefin.* **2023**, *13*, 2487.

[32] T. Tang, B. Zhang, X. Liu, W. Wang, X. Chen, B. Fei, *Sci. Rep.* **2019**, *9*, 12824.

[33] D. S. de Sá, E. J. da Rocha Rodrigues, N. M. Suguihiro, A. G. da Veiga, S. Paciornik, A. Massi, O. G Pandoli, *Catal. Lett.* **2022**, *152*, 3558.

[34] B. G. Palma, R. A. C. Leão, R. O. M. A. de Souza, O. G. Pandoli, *Catal. Today* **2021**, *381*, 280.

[35] L. O. L. Gontijo, M. N. B. Junior, D. Santos de Sá, S. Letichevsky, M. J. Pedrozo-Peñafiel, R. Q. Aucélio, I. S. Bott, H. Diniz Lopes Alves, B. Fragneaud, I. Oliveira Maciel, A. Linhares Rossi, L. Savio, G. Carraro, A. Anja, F. Lazaro Freire, G. Khosrow, S. Paciornik, O. Ginoble Pandoli, *Carbon* **2023**, *213*, 118214.

[36] O. G Pandoli, R. S. Martins, K. L. G. De Toni, S. Paciornik, M. H. P. Maurício, R. M. C. Lima, N. B. Padilha, S. Letichevsky, R. R. Avillez, E. J. R. Rodrigues, K. Ghavami, *J. Coat. Technol. Res.* **2019**, *16*, 999.

[37] C.-M. Kuan, R. L. York, C.-M. Cheng, *Sci. Rep.* **2015**, *5*, 18570.

[38] M. Su, R. Zhang, J. Li, X. Jin, X. Zhang, D. Qin, *Cellulose* **2021**, *28*, 11713.

[39] J. Li, R. Ma, Y. Lu, Z. Wu, R. Liu, M. Su, X. Jin, R. Zhang, Y. Bao, Y. Chen, D. Qin, D. Yang, Z. Jiang, *Appl. Catal., B* **2022**, *310*, 121297.

[40] C. Liu, S. Zhang, S. Yan, M. Pan, H. Huang, *Forests* **2024**, *15*, 371.

[41] F. Suryani, T. Rihayat, Nurhanifa, T. Y. R. Hasnah, *IOP Conf. Ser. Mater. Sci. Eng.* **2020**, *854*, 012050.

[42] A. Maurya, M. K. Singh, S. Kumar, in *Waterborne Pathogens: Detection and Treatment* (Eds.: M. N. Vara Prasad, A. Grobelak), Elsevier, Amsterdam **2020**, pp. 123–141.

[43] R. Rotaru, M. Savin, N. Tudorachi, C. Peptu, P. Samoila, L. Sacarescu, V. Harabagiu, *Polym. Chem.* **2018**, *9*, 860.

[44] P. Ahvenainen, I. Kontro, K. Svedström, *Cellulose* **2016**, *23*, 1073.

[45] L. Segal, J. J. Creely, A. E. Martin, C. M. Conrad, *Text. Res. J.* **1959**, *29*, 786.

[46] X. Li, H. C. Li, T. T. You, Y. Y. Wu, S. Ramaswamy, F. Xu, *Ind. Crops Prod.* **2019**, *140*, 111603.

[47] D. Meroni, L. L. Presti, G. Di Liberto, M. Ceotto, R. G. Acres, K. C. Prince, R. Bellani, G. Soliveri, S. Ardizzone, *J. Phys. Chem. C* **2017**, *121*, 430.

[48] M. Sypabekova, A. Hagemann, D. Rho, S. Kim, *Biosensors* **2022**, *13*, 36.

[49] V. Hodoroaba, S. Rades, P. Borghetti, E. Ortel, T. Wirth, S. García, E. Gómez, M. Blanco, G. Alberto, G. Martra, *Surf. Interface Anal.* **2020**, *52*, 829.

[50] B. Díaz de Greñu, S. Muñoz-Pina, R. de los Reyes, M. Benitez, J. El Haskouri, P. Amorós, J. V. Ros-Lis, *ChemSusChem.* **2023**, *16*, e202300123.

[51] F. Bauer, S. Czihal, M. Bertmer, U. Decker, S. Naumov, S. Wassersleben, D. Enke, *Microporous Mesoporous Mater.* **2017**, *250*, 221.

[52] J. M. Kremsner, C. O. Kappe, *Eur. J. Org. Chem.* **2005**, *2005*, 3672.

[53] D. Dallinger, C. O. Kappe, *Chem. Rev.* **2007**, *107*, 2563.

[54] R. M. Pasternack, S. Rivillon Amy, Y. J. Chabal, *Langmuir* **2008**, *24*, 12963.

[55] Q. Ding, W. Han, X. Li, Y. Jiang, C. Zhao, *Sci. Rep.* **2020**, *10*, 21387.

[56] T. Yamashita, K. Takatsuka, *J. Chem. Phys.* **2007**, *126*, 074304.

[57] T. Afrin, R. K. Kanwar, X. Wang, T. Tsuzuki, *J. Text. Inst.* **2014**, *105*, 1293.

**ADVANCED
SCIENCE NEWS**

www.advancedsciencenews.com

**ADVANCED
SUSTAINABLE
SYSTEMS**

www.advsustainsys.com

[58] X. Li, Y. Wei, J. Xu, N. Xu, Y. He, *Biotechnol. Biofuels* **2018**, *11*, 263.

[59] P. J. Larkin, in *Infrared and Raman Spectroscopy: Principles and Spectral Interpretation*, Elsevier, Amsterdam **2018**, pp. 29–61.

[60] A. Koçak, W. Wyatt, M. A. Comanescu, *Forensic Sci. Int.* **2021**, *328*, 111002.

[61] E. Leng, Y. Zhang, Y. Peng, X. Gong, M. Mao, X. Li, Y. Yu, *Fuel* **2018**, *216*, 313.

[62] J. A. Sirviö, M. Lakovaara, *Biomacromolecules* **2021**, *22*, 3366.

[63] Z. Ba, H. Luo, J. Guan, J. Luo, J. Gao, S. Wu, R. O. Ritchie, *Nat. Commun.* **2023**, *14*, 1234.

[64] J. Wei, C. Du, H. Liu, Y. Chen, H. Yu, Z. Zhou, *BioResources* **2016**, *11*, 8386.

[65] D. D. Miller, M. W. Smith, D. Shekhawat, *J. Phys. Chem. Solids* **2021**, *150*, 109858.

[66] M. Sadeghi-Shapourabadi, S. Elkoun, M. Robert, *Macromol.* **2023**, *3*, 766.

[67] W. Fatriasari, W. Syafii, N. Wistara, K. Syamsu, B. Prasetya, *Int. J. Adv. Sci. Eng. Inf. Technol.* **2016**, *6*, 187.

[68] L. M. Bal, Yogranjan, S. N. N, S. Satya, A. Kar, *J. Food Meas. Charact.* **2017**, *11*, 1203.

[69] Y. Wang, H. Shao, H. Pan, Y. Jiang, J. Qi, Q. Chen, S. Zhang, H. Xiao, Y. Chen, S. Jia, X. Huang, L. Tu, Z. Su, J. Xie, *Int. J. Biol. Macromol.* **2023**, *230*, 123251.

[70] K. Kulasinski, S. Keten, S. V. Churakov, D. Derome, J. Carmeliet, *Cellulose* **2014**, *21*, 1103.

[71] K. Daicho, T. Saito, S. Fujisawa, A. Isogai, *ACS Appl. Nano Mater.* **2018**, *1*, 5774.

[72] S. Park, J. O. Baker, M. E. Himmel, P. A. Parilla, D. K. Johnson, *Biotechnol. Biofuels* **2010**, *3*, 10.

[73] N. T. Hamdan, *Syst. Rev. Pharm.* **2020**, *11*, 6.

[74] A. Garcia-Maraver, D. Salvachúa, M. J. Martínez, L. F. Diaz, M. Zamorano, *Waste Manage.* **2013**, *33*, 2245.

[75] J. Wang, E. Minami, H. Kawamoto, *J. Wood Sci.* **2020**, *66*, 41.

[76] C. P. Azubuike, J. O. Odulaja, A. O. Okhamafe, *J. Excipients Food Chem.* **2012**, *3*, 106.

[77] H. Khanjanzadeh, R. Behrooz, N. Bahramifar, W. Gindl-Altmutter, M. Bacher, M. Edler, T. Griesser, *Int. J. Biol. Macromol.* **2018**, *106*, 1288.

[78] M. S. Bertran, B. E. Dale, *J. Appl. Polym. Sci.* **1986**, *32*, 4241.

[79] S. M. L. Rosa, N. Rehman, M. I. G. De Miranda, S. M. B. Nachtigall, C. I. D. Bica, *Carbohydr. Polym.* **2012**, *87*, 1131.

[80] E. Robles, L. Csóka, J. Labidi, *Coatings* **2018**, *8*, 139.

[81] K. S. Salem, N. K. Kasera, M. A. Rahman, H. Jameel, Y. Habibi, S. J. Eichhorn, A. D. French, L. Pal, L. A. Lucia, *Chem. Soc. Rev.* **2023**, *52*, 6417.

[82] A. Alemdar, M. Sain, *Bioresour. Technol.* **2008**, *99*, 1664.

[83] J. Luo, C. Lian, R. Liu, S. Zhang, F. Yang, B. Fei, *Sci. Rep.* **2019**, *9*, 10876.

[84] X. Gao, D. Zhu, S. Fan, M. Z. Rahman, S. Guo, F. Chen, *J. Mater. Res. Technol.* **2022**, *19*, 1162.

[85] F. Guo, X. Zhang, R. Yang, L. Salmén, Y. Yu, *Cellulose* **2021**, *28*, 8867.

[86] J. Wu, T. Zhong, W. Zhang, J. Shi, B. Fei, H. Chen, *J. Wood Sci.* **2021**, *67*, 56.

[87] R. Ramful, T. P. M. Sunthar, K. Kamei, G. Pezzotti, *Antibiotics* **2022**, *11*, 569.

[88] N. Gokarneshan, *Biomed. J. Sci. Tech. Res.* **2020**, *32*, 25299.

[89] L. Xi, D. Qin, X. An, G. Wang, *BioResources* **2013**, *8*, 6501.

[90] A. Alzagameem, S. E. Klein, M. Bergs, X. T. Do, I. Korte, S. Dohlen, C. Hüwe, J. Kreyenschmidt, B. Kamm, M. Larkins, M. Schulze, *Polymers* **2019**, *11*, 670.

[91] M. K. Mandal, A. J. Domb, *Pharmaceutics* **2024**, *16*, 718.

[92] A. Carmona-Ribeiro, L. De Melo Carrasco, *Int. J. Mol. Sci.* **2013**, *14*, 9906.

[93] H. Luo, Y. Z. Jiang, L. Tan, *J. Hazard. Mater.* **2022**, *424*, 127299.

[94] T. J. Silhavy, D. Kahne, S. Walker, *Cold Spring Harbor Perspect. Biol.* **2010**, *2*, a000414.

[95] A. Hassanpour, S. Asghari, M. M. Lakouraj, *RSC Adv.* **2017**, *7*, 23907.

[96] A. Hassanpour, S. Asghari, M. Mansour Lakouraj, M. Mohseni, *Int. J. Biol. Macromol.* **2018**, *115*, 528.

[97] P. Sperandeo, F. Bosco, F. Clerici, A. Polissi, M. L. Gelmi, A. Romanelli, *ACS Appl. Bio Mater.* **2020**, *3*, 4895.

[98] E. O. Carvalho, M. Rincón-Iglesias, R. Brito-Pereira, E. Lizundia, M. M. Fernandes, S. Lanceros-Mendez, *Int. J. Biol. Macromol.* **2023**, *242*, 125049.

[99] T. Serizawa, S. Yamaguchi, K. Sugiura, R. Marten, A. Yamamoto, Y. Hata, T. Sawada, H. Tanaka, M. Tanaka, *ACS Appl. Bio Mater.* **2024**, *7*, 246.

[100] X.-Y. Ye, E.-Q. Zhu, D.-W. Wang, J. Yang, H.-Y. Yang, Z.-J. Shi, *Ind. Crops Prod.* **2022**, *188*, 115607.

[101] B. Szadkowski, A. Marzec, M. Kuśmierek, M. Piotrowska, D. Moszyński, *Int. J. Biol. Macromol.* **2024**, *259*, 129178.

[102] J. Li, Z. Wang, H. Xiu, X. Zhao, F. Ma, L. Liu, C. Yi, M. Zhang, E. Kozliak, Y. Ji, *Powder Technol.* **2022**, *399*, 117194.

[103] W. Yanming, C. Zhongjia, Y. Xiangyue, Y. Guosheng, *Wood Res.* **2018**, *63*, 655.

[104] S. Tasnim, M. F. K. Tipu, M. S. Rana, M. A. Rahim, M. Haque, M. S. Amran, A. A. Chowdhury, J. A. Chowdhury, *Materials* **2023**, *16*, 5664.

[105] S. C. Esparza-González, S. Sánchez-Valdés, S. N. Ramírez-Barrón, M. J. Loera-Arias, J. Bernal, H. I. Meléndez-Ortiz, R. Betancourt-Galindo, *Toxicol. In Vitro* **2016**, *37*, 134.